International Journal of Fluid Power 8 (2007) No. 2 pp. 5-16

ELECTRONIC CONTROL OF PUMP PRESSURE FOR A SMALL HAPTIC BACKHOE

Matthew E. Kontz[1] and Wayne J. Book[2]

[1]*Caterpillar Inc. – Technology and Solutions Division – Hydraulics Research, Peoria, IL, USA*
[2]*Georgia Institute of Technology – G. W. Woodruff School of Mechanical Engineering, Atlanta, GA, USA*
Kontz_Matthew_E@cat.com, wayne.book@me.gatech.edu

Abstract

The use of haptic interfaces to control mobile hydraulic machinery has several enhancing features over traditional human-machine interfaces comprised of joysticks/levers. This paper presents and analyzes schemes for controlling pump pressure designed for coordinated haptic control. Typical of many small backhoes and excavators, the hydraulic system used on the test-bed is comprised of a constant displacement pump and proportional directional control valves. In this type of system, a main pressure regulator is needed to supply the other closed-centre valves with pressure and to dump the additional flow generated by the pump to tank. An energy-saving solution has a load-sensing pressure regulator that maintains the system pressure to a preset margin above the highest active load pressure. Using these valves for haptic applications requires closed-loop control. Applying closed-loop control to these valves can excite instabilities in the valve assembly due to complex interactions and nonlinearities in the load-sensing pressure regulator and proportional valves. On this setup, the hydro-mechanical pressure regulator has been replaced with one that is electronically controlled, and a non-linear filter is utilized to decouple oscillations in port pressure from the pump pressure input signal. This filter does not slow down the build up of pump pressure. Experimental results with multiple degrees-of-freedom are presented.

Keywords: haptics, excavators, backhoes, coordinated motion, electronic load sensing, pressure control

1 Introduction

The definition of haptics is *of or relating to the sense of touch or tactile*. Haptic control implies that the human-machine interface can be programmed to artificially supply the user with arbitrary force sensations. Typically the haptic forces are used to relay information about the forces acting on a remote or virtual environment. A haptic interface offers several possible enhancements other than force reflection. These devices enable coordinated motion control and the ability to program virtual fixtures (Kontz et al., 2005a; Rosenberg, 1993) into the workspace. Coordinated control is a subtle, but profound, improvement over conventional hand controllers that work in joint space. Using joysticks that individually control the joints of the manipulator puts a "high perceptual and psychomotor demand" on the operator (Wallersteiner et al., 1988; Wallersteiner et al., 1993). Using coordinated motion control and a single hand controller whose motion corresponds directly to the slave manipulator reduces this mental load by doing the inverse kinematics for the operator.

The primary goal of this project is to explore how haptic interfaces can enhance the ability of novice and expert operators to control hydraulic machinery such as backhoe-loaders and hydraulic excavators. However, the focus of this paper is the hydraulic control system that will later be used for closed-loop haptic control. While hydraulic systems offer a practical application of haptic feedback, their characteristics can create control challenges. In the case of proportional directional control valves these characteristics include nonlinear valve orifice coefficients, delay, dead-band and slow dynamics. When implemented on mobile equipment, dynamics associated with the pump and primary pressure/flow control must also be considered. Closing the loop on these dynamics can also cause instabilities.

The valve dead-band is an issue of concern when closing the loop around a proportional directional con-

This manuscript was received on 21 February 2007 and was accepted after revision for publication on 6 June 2007

trol valve. One way to deal with dead-band is to use a dead-band inverse in the control. In the case of a servo valve with fast dynamics, this can be achieved with good performance (Fortgang et al., 2002). Regardless of their cost, servo valves are not well suited for mobile application due to their sensitivity to contamination. In the case of proportional valves the effectiveness of the dead-band inverse is limited by the dynamics of valves (Liu and Yao, 2004; Taware et al., 2002). This is due to the dead-band nonlinearity being sandwiched between the spool dynamics and the dynamics of the rest of the hydraulic system. The inverse dead-band is located at the input and corrects the desired spool position; however, the limitation on how fast the spool can move determines how fast the desired spool position can be achieved. In turn, this limits how well the system can track a desired trajectory. One way to minimize the effect of spool dead-band and improve overall performance is to increase the responsiveness of the spool control stage. Tafazoli et al. (1996) created a custom differential PWM pilot stage that could move the spool faster in order to improve the responsiveness of the main spool used on their haptic mini-excavator.

Another factor that can limit how fast a system responds is the rate at which the main system pressure can build up (Lee and Chang, 2001). This is especially true of load-sensing systems that react to the maximum line pressures of any of the open valves. This type of design is good from an energy savings point of view, but is detrimental to closed-loop control, which is necessary for haptic teleoperation (Krishnaswamy and Li, 2006; Salcudean et al., 1999; Tafazoli et al., 2002) or autonomous operation (Ha et al., 2002; Stentz et al., 1998; Vaha and Skibniewski, 1993). The system has to wait in order for pressure to build up when starting from rest and the pressure can drop and may need to build up again when the valve orifices are temporarily closed as the valves change the direction of the flow. This problem could be minimized by using a pressure regulating valve with an electronically controlled set point. The pressure can then be built up as the spool moves through the dead-band.

Another factor that can compound this problem is that the pilot pressure that is used by the main spool is supplied from a pressure reducing valve that is fed by the main system pressure. When all the spools are in the dead-band region, the main system pressure drops below the set point of the pressure reducing valve. Due to this, the spool pilot pressure drops along with the responsiveness of the spool.

From an energy and performance standpoint, being able to optimize the pressure of the system is particularly important on this type of system. Typically, larger equipment such as backhoe-loaders and hydraulic excavators have variable displacements pump(s) and a separate pilot system. The variable displacement pump allows both pump flow(s) and pressure(s) to follow the demands of the task. Having a separate pilot system allows the main pump pressure to drop to a very low pressure without reducing the pilot pressure. These features are less likely to be installed on smaller machines such as this tractor mounted backhoe and mini-excavators due to hardware cost and size constraints.

Flow allocation must also be considered. The main pressure regulator is essentially a pressure relief valve that is modulating the pressure of the system. Three different pressure regulating configurations are explored: the original hydro-mechanical load-sensing pressure regulator, a constant pressure relief valve and an electronic load-sensing pressure relief valve. One thing that all three of these configurations have in common is that if they are not bypassing any flow then they are not able to regulate the system pressure. This can be solved by limiting the flow commanded by the controller.

The focus of this paper is on controlling the pump pressure for coordinated motion using multiple cylinders. This work builds on work presented by Kontz et al. (2005b). The coordinated velocity/flow scheme is discussed in more detail in Kontz and Book (2007). In the following section the experimental setup is described. In Section 3, the system is described and the dynamic interactions are analyzed. In Section 4, the importance of flow limiting control is presented and in Section 5 a nonlinear filter designed to decouple the system is presented and pressure control with multiple cylinders is demonstrated.

2 Experimental Setup

Fig. 1: *Georgia Tech's haptic backhoe test-bed*

The primary test-bed in this project is referred to as HEnRE (Haptically ENhanced Robotic Excavator) (Frankel, 2004) and is based around a 4410 series John Deere tractor with a Model 47 backhoe and a PHANToM (Massie and Salisbury, 1994) haptic display built commercially by SensAble Technologies. The Model 47 backhoe has been modified. Originally, manual valves were the only means available to operate the device. Flow is supplied from a constant displacement pump. It has been retrofitted with Sauer-Danfoss PVG-32/PVES electro-hydraulic (EH) valves and an array of sensors for feedback control and monitoring.

A mechanical valve is used to switch between the original valves and the retro-fitted EH valves. A Sun Hydraulics RPEC-8WN/RBAP-MAN-224 electro-proportional pressure relief valve was added for electronic pressure control. Instrumentation installed on HEnRE includes: position of all four degrees of freedom

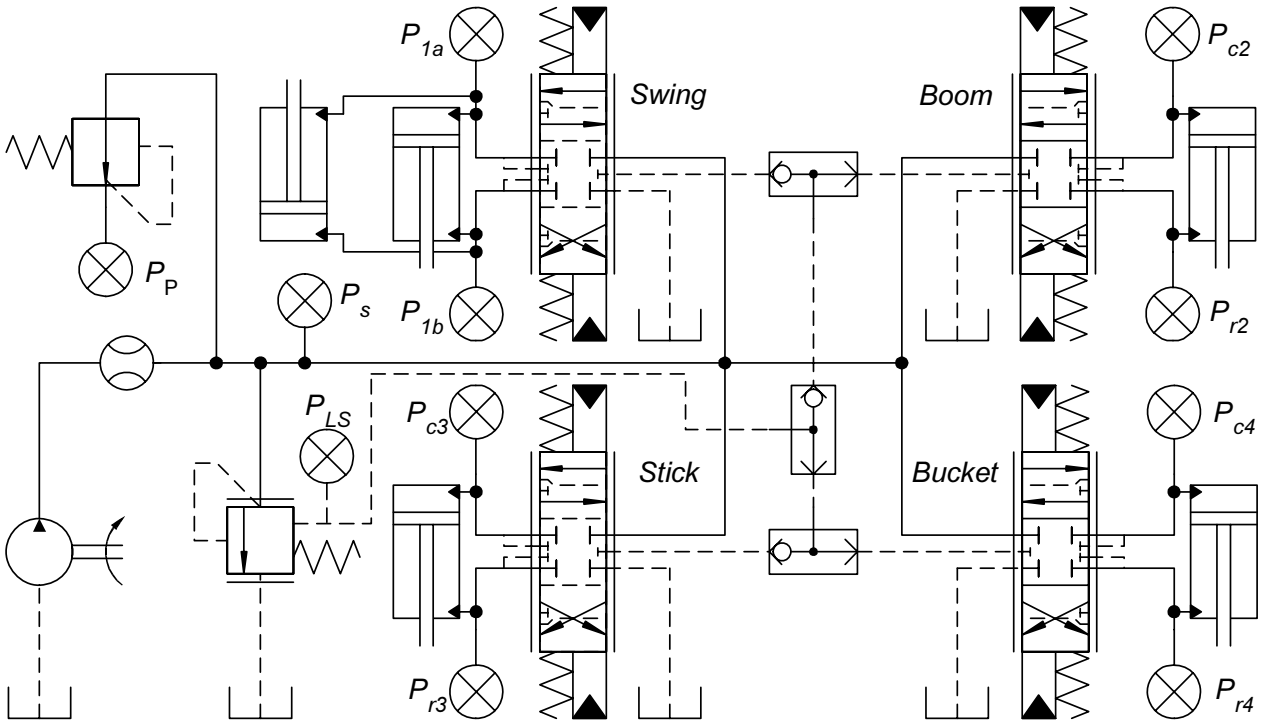

Fig. 2: *Schematic of the overall PVG-32/PVES system with hydro-mechanical load-sensing control of the pressure relief valve regulating pump pressure, P_s. A pressure reducing valve is used to regulate the pilot pressure, P_p, which is used by the electro-hydraulic proportional spool control stages show in Fig. 3*

(swing, boom, stick and bucket), capside pressures, rodside pressures, system/pump pressure, load-sense pressure, pump flow and inlet oil temperature. The control software for the backhoe is based on Mathwork's xPC target. This real-time control software interfaces with another computer controlling the PHANToM via Ethernet cable using UDP protocol. PHANToM control is implemented in a Windows operating system using SensAble's C++ software libraries.

3 Hydraulic System

The schematic of the hydraulic system is shown in Fig. 2. Four Sauer-Danfoss PVG-32 proportional valves are used to regulate the flow going to the four degrees of freedom of the backhoe. These valves are designed to be controlled by electronic joysticks for use in mobile hydraulic applications. They are designed to deliver a steady-state flow proportional to the input voltage signal with the addition of pressure compensators making them ideal for this application. These valves can be stacked and can operate with a constant displacement pump with the addition of a main pressure regulator to control pump pressure. The main pressure regulator is essentially a pressure relief valve that is modulating the system or pump pressure, P_s, and bypassing all the extra flow back to tank. At the same time the individual closed-centre proportional valves can hold the actuators in place while the valves are in their neutral position. Each PVG-32/PVES module has two major components: main spools and pilot spool controllers (PVES modules). The main spools and pilot spool controllers are discussed in Section 3. 1 and three different pressure regulating schemes are described in Section 3.2.

3.1 Proportional Control Valves

The flow going to each cylinder is changed by moving the spool back and forth in order to adjust the orifice size between one port and tank and another orifice between the opposite port and the pump pressure, P_s. When a neutral signal is given to the valves the spool centres itself so that the overlap in the spool prevents internal leakage. It is this overlap that causes the deadband in the system. These orifices can be described using a standard orifice equation (Merritt, 1967). The relationship between flow, Q, and pressure drop across the orifice, ΔP, can be described in general using the following equation.

$$Q = C_d A_0 \sqrt{\frac{2}{\rho}\Delta P} = K_q(x_{xp}, T)\sqrt{\Delta P} \qquad (1)$$

Where C_d is the discharge coefficient and A_0 is the orifice area. The combined term $C_d A_0$ is a function of spool position, x_{sp}, because the area and shape of the orifice change as the spool moves. As the temperature increases, the density, ρ, decreases and C_d increases due to a decrease in viscosity of the oil. Both of these factors result in more flow for the same pressure drop. The effect of oil temperature is ignored. For controller simplicity, it is assumed that flow is only a function of pressure drop and spool position.

$$Q_c = \text{sign}(\Delta P_c) K_{qc}(x_{sp}, T)\sqrt{|\Delta P_c|} \quad (2)$$

$$Q_r = \text{sign}(\Delta P_r) K_{qr}(x_{sp}, T)\sqrt{|\Delta P_r|} \quad (3)$$

Valve orifice flow coefficients, K_{qc} and K_{qr}, control the flow going in and out of the capside and rodside of the cylinder. The pressure drop, ΔP, is measured across the valve orifice from the system pressure to port or tank to port. Pressure compensators can also be used to linearize the relationship between input voltage versus steady-state flow. Pressure compensators are used to regulate the pressure drop across the orifice receiving flow from the pump. This can be beneficial since the compensators can adjust to changes in pressure faster than the closed-loop dynamics of the spool.

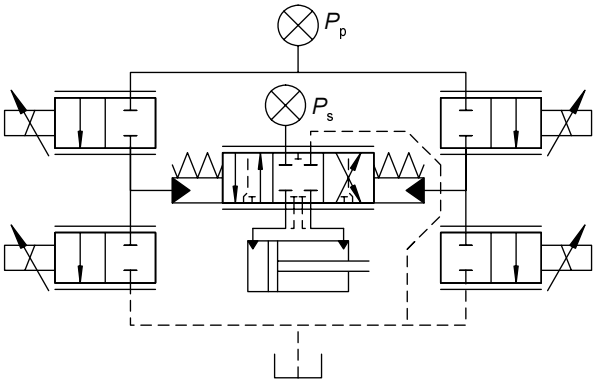

Fig. 3: *Block diagram of Sauer-Danfoss PVG32/PVES spool position controller. The pilot pressure, P_p, is controlled by the pressure reducing valve in Fig. 2. The four solenoids in the wheatstone bridge are controlled by a 40 Hz PWM (pulse width modulated) signal*

The PVG-32 spools are modulated using the PVES electronically controlled spool stages. This stage design is shown in Fig. 3. Four small solenoid valves are arranged in a wheatstone bridge configuration in order to move the main spool back and forth. This wheatstone bridge is supplied with pressure and flow from a pressure reducing valve shown in Fig. 2. The solenoid valves are modulated using a PWM (pulse width modulated) signal at 40 Hz. The dynamics between the input voltage, V_{in}, and the spool position, x_{sp}, can be approximated for low frequencies using a second order system with a pure delay element. This delay is likely a result of the 40 Hz frequency of the PWM controller.

$$\frac{X_{sp}}{V_{in}} = \frac{k\omega_n^2 e^{-\tau s}}{s^2 + 2\zeta\omega_n s + \omega_n^2} = \frac{0.436 \cdot 1947 e^{-0.0125 s}}{s^2 + 62.1 s + 1947} \quad (4)$$

Experimental results indicate that Eq. 4 is a good approximation for system pressures above about 2.06 MPa (300 psi). In this range the bandwidth of the spool control stage is around 7-8 Hz and the damping ratio is about 0.7. The actual dynamics vary with oil temperature and pump pressure, P_s. If pump pressure is below this range the bandwidth of the spool significantly drops off. This is because the pressure reducing valve regulating P_p is not properly pressurized. This is consistent with the fact that the pressure reducing valve regulates the pilot pressure used by the spool stage at 1.5 MPa (217 psi).

If all the main valves are closed or moving through the dead-band region, the system pressure drops to its minimum pressure around 1.03 - 1.38 MPa (150 - 200 psi) because none of the ports are pressurizing the load-sense pressure line. Experimental results show that it takes longer for the spool to pass through the spool's dead-band region when the system pressure and therefor pilot pressure is too low. Normally, it would take about 50ms to pass through the valve dead-band. When the system pressure and therefore the pilot pressure drop, the 50ms dead-band crossing time increases to as much as 110ms.

3.2 Main Pressure Regulator Designs

Three different pressure regulator designs are used in these experiments: a hydro-mechanical load-sensing pressure regulator, a hydro-mechanical constant pressure regulator and an electronically controlled pressure regulator.

3.2.1 Hydro-Mechanical Regulation

The main pressure regulator is essentially a pressure relief valve that opens to tank when the system pressure, P_s, surpasses some value. The system pressure is then used by the individual proportional valves that operate each degree of freedom. With load-sensing enabled, the pressure regulator tries to maintain P_s a constant pressure margin, P_{margin}, above the load-sense pressure, P_{LS}. The load-sense pressure is driven by the maximum pressure of the ports receiving flow from the pump. These spools are designed to open the port pressures to the load-sense line right before they move enough to create a control orifice. This is good from an energy savings point of view, but it adds delay to the system. The relationship between P_s and P_{LS} can be approximated by the following experimentally derived transfer function.

$$\frac{P_s(s)}{P_{LS}(s) + P_{margin}} = \frac{1}{\tau_{P_s} s + 1} \quad (5)$$

The pressure margin, P_{margin}, is around 1.05 MPa \ (153 psi) and the experimental time constant, τ_{Ps}, is around 0.012 seconds (12.6 Hz). The pressure margin is the minimum pressure differential between the pump pressure and the load-sensing pressure. It also sets the minimum pressure drop across the control orifices of the proportional valves. It is set by the force balance on the pressure relief valve. There is also a dynamic relationship between the port pressures and the load-sense pressure. For each degree of freedom

$$P_{LS_i} = \begin{cases} P_c & i^{th}\ cylinder\ is\ extending \\ P_{min} \neq 0 & i^{th}\ cylinder\ in\ deadband \\ P_r & i^{th}\ cylinder\ is\ retracting \end{cases} \quad (6)$$

Only the largest of the four P_{LSi} signals drive the load-sense pressure and the main system pressure. The maximum pressure is selected using a series of shuttle valves (Fig. 2). There is also a dynamic relationship

between the maximum P_{LSi} and P_{LS}.

$$\frac{P_{LS}(s)}{\max\left\{P_{LS_{1\text{-}4}}\right\}(s)} = \frac{1}{\tau_{LS}s+1} \tag{7}$$

This experimental time constant, τ_{LS}, is equal to 0.018 seconds (8.9 Hz). This model was derived empirically, but it is similar to a pressure valve model derived analytically by Kappi and Ellman (2000).

3.2.2 Constant Pressure Regulation

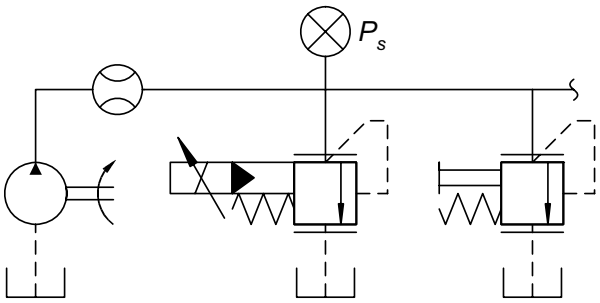

Fig. 4: *The relief valve on the left is the external electro-proportional relief valve. The second relief valve is the same relief valve shown in Fig. 2 that is built into the PVG-32 assembly; however, in this diagram the load-sensing is disabled. With both relief valves installed, the valve with the lower setting will control the system pressure*

The relief valve located inside the Sauer-Danfoss PVG-32 assembly can be converted into a constant pressure relief valve by replacing a plug/orifice with a plug that blocks off the load-sensing network. In this configuration, the main pressure relief valve located inside the PVG-32 valve assembly maintains the pressure below a manually adjustable constant value. This also enables an external pressure valve to control the main pressure. When both the internal and external pressure relief valves shown in Fig. 4 are installed at the same time, only the one with the lower pressure setting has any affect on the system pressure.

3.2.3 Electro-proportional Regulation

Electronic load-sensing pressure control can be achieved using the external electro-hydraulic pressure relief valve shown in Fig. 4. This adds flexibility to how the main system pressure is controlled. For example, the pressure minimum can be set such that the pilot pressure is high enough to assure maximum spool responsiveness. It also allows pressure to be built up or held constant while the spool is moving through the dead-band. These changes in how the pressure is controlled can improve the responsiveness of these valves. At the same time, the energy efficiency is still better than if the system pressure was held at a constant value. Using the electro-proportional relief valve enables the system pressure to be varied for efficiency without sacrificing smoothness or responsiveness.

3.3 Dynamic Pressure Coupling

Using a hydro-mechanical load-sensing system to control pump pressure results in dynamic coupling between the states of each cylinder and the pump pressure. This can be seen graphically in Fig. 5.

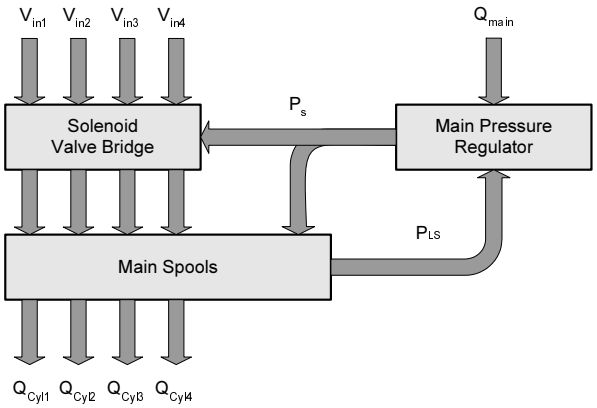

Fig. 5: *Block Diagram of the hydro-mechanical load-sensing pressure regulator built into the PVE/PVG32 assembly*

A deeper understanding is possible by modeling the pump and cylinder states, linearizing and putting them in state-space form. In this model it is assumed that the cylinder is retracting and receiving flow from the pump on the rodside of the cylinder. If this was the boom degree of freedom, this would correspond to raising the boom with all other functions not moving. For the following equations this would mean that θ was equal to the boom joint angle, θ_2 and x_c was equal to the boom cylinder length, y_{c2} (Fig. 6).

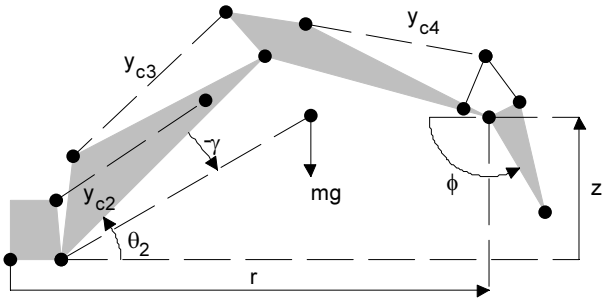

Fig. 6: *Cylinder-space and task-space variables. The centroid and gravitational force is also shown for the last three links assuming the third and fourth cylinders are locked*

Starting with the general rigid body equation.

$$J\ddot{\theta} + G(\theta) = \tau = \frac{\partial x_c}{\partial \theta} F_c \tag{8}$$

Note that the joint torque, τ, can be related to cylinder force, F_c, via the joint angle to cylinder length Jacobian (Kontz and Book, 2006). An equivalent mass in the cylinder domain, m_{eq}, can be found by expressing the kinetic energy, KE, in terms of the time derivatives of both θ and x_c.

$$KE = \frac{1}{2}J\dot{\theta}^2 = \frac{1}{2}J\left(\frac{\partial x_c}{\partial \theta}\dot{x}_c\right)^2 = \frac{1}{2}m_{eq}\dot{x}_c^2 \tag{9}$$

Using cylinder variables the dynamic equation becomes

$$m_{eq}\ddot{x}_c = -\frac{\partial \theta}{\partial x_c}G\left(\theta\left(x_c\right)\right) + F_c \tag{10}$$

where

$$G\left(x_c\right) = mgl\cos\left(\theta\left(x_c\right)+\gamma\right) \tag{11}$$

Assuming a viscous-Coulomb friction model

$$F_c = A_c P_c - A_r P_r - \text{sign}\left(\dot{x}_c\right)F_{coul} - b_v\dot{x}_c \tag{12}$$

The pressure derivatives are modeled based on the compressibility in the volume of fluid between the valves and cylinder. The equivalent bulk modulus, B_e, includes air in the oil, air pockets and expansion of the hoses.

$$\dot{P}_c = \frac{B_e}{V_c}\left(-A_c\dot{x}_c + K_{sp}\left(x_{sp}\right)\sqrt{P_c}\right) \tag{13}$$

$$\dot{P}_r = \frac{B_e}{V_r}\left(A_r\dot{x}_c - K_{sp}\left(x_{sp}\right)\sqrt{P_s - P_r}\right) \tag{14}$$

where

$$K_{sp}\left(x_{sp}\right) = k\left(x_{sp} - \text{sign}\left(x_{sp}\right)\right) \tag{15}$$

It is assumed that the orifice coefficient, K_{sp}, is linear with spool position, x_{sp}, when x_{sp} is outside of the dead-band region around zero. The tildes on the following state vector and the state variables represent that they are relative to the nominal values of the linearization. The nominal values are denoted by over bars.

$$\tilde{\boldsymbol{X}} = \left[\tilde{x}_c\ \dot{\tilde{x}}_c\ \tilde{x}_{sp}\ \dot{\tilde{x}}_{sp}\ \tilde{P}_c\ \tilde{P}_r\ \tilde{P}_s\ \tilde{P}_{LS}\right] \tag{16}$$

The linear state space equation is found by linearizing Eq. 4, 5, 7, 10, 13 and 14 for a given position and velocity of the cylinder.

$$\dot{\tilde{\boldsymbol{X}}} = \mathbf{A}\,\tilde{\boldsymbol{X}} + \boldsymbol{B}\tilde{V}_{in} \tag{17}$$

The state matrix is:

$$\mathbf{A} = \begin{bmatrix} 0 & 1 & 0 & 0 & 0 & 0 & \vdots & 0 & 0 \\ c_1 & -\frac{b_v}{m_{eq}} & 0 & 0 & \frac{A_c}{m_{eq}} & -\frac{Ar}{m_{eq}} & \vdots & 0 & 0 \\ 0 & 0 & 0 & 1 & 0 & 0 & \vdots & 0 & 0 \\ 0 & 0 & -\omega_n^2 & -2\zeta\omega_n & 0 & 0 & \vdots & 0 & 0 \\ 0 & \mu_c A_c & \mu_c k_{sp}\sqrt{\bar{P}_c} & 0 & \frac{\mu_c K_{sp}\left(\bar{x}_{sp}\right)}{2\sqrt{\bar{P}_c}} & & \vdots & 0 & 0 \\ 0 & \mu_r A_r & c_2 & 0 & 0 & c_3 & \vdots & -c_3 & 0 \\ \cdots & \cdots & \cdots & \cdots & \cdots & \cdots & & \cdots & \cdots \\ 0 & 0 & 0 & 0 & 0 & 0 & \vdots & -\frac{1}{\tau_{P_s}} & \frac{1}{\tau_{P_s}} \\ 0 & 0 & 0 & 0 & 0 & \frac{1}{\tau_{P_{LS}}} & \vdots & 0 & -\frac{1}{\tau_{P_{LS}}} \end{bmatrix} \tag{18}$$

where,

$$\mu_c = \frac{B_e}{V_c}, \quad \mu_r = \frac{B_e}{V_r} \tag{19}$$

$$c_1 = \frac{mgl}{J}\sin\left(\theta\left(\bar{x}_c\right)+\gamma\right) \tag{20}$$

$$c_2 = -\mu_r k_{sp}\sqrt{\bar{P}_s - \bar{P}_r} \tag{21}$$

$$c_3 = \frac{\mu_r K_{sp}\left(\bar{x}_{sp}\right)}{2\sqrt{\bar{P}_s - \bar{P}_r}} \tag{22}$$

The input matrix is:

$$\boldsymbol{B} = \left[0\ \ 0\ \ 0\ \ \omega_n^2\ \ 0\ \ 0\ \ 0\ \ 0\right]^T \tag{23}$$

In this state vector the first six states are associated with the specific cylinder and the last two are associated with the pump pressure. The pump pressure states are coupled to the dynamics of the cylinders in two ways. The first is through the port pressure receiving flow from the pump. In general when multiple functions are used this ties the pump directly to the pressures of all the ports receiving flow from the pump. For the one cylinder case shown in Eq. 18 this coupling is shown by the coefficient "-c_3." The other coupling is from the port pressure that is driving the load-sensing state. This is shown in Eq. 18 by the "$1/\tau_{P_{LS}}$" term.

This means that if the pressure driving the load-sensing pressure causes P_s to change, then both the port pressures and spool positions have to change in order to maintain the desired cylinder motion. This is troublesome if the port pressure driving the load-sensing becomes oscillatory. The closed-loop bandwidth of the spool is also slower than the speed of the pressure change.

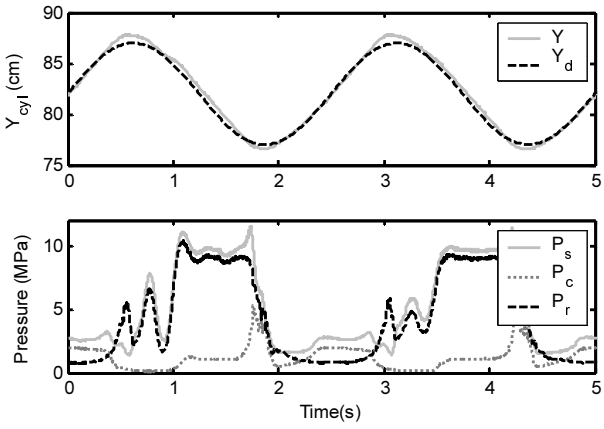

Fig. 7: *Hydro-mechanical loading-sensing pressure regulation*

This problem is demonstrated by the data in Fig. 7. The boom is given a sine trajectory. Y and Y_d are the actual and desired cylinder lengths. P_s, P_c and P_r are system, capside and rodside pressures. When the pressure needs to increase for the boom to rise (cylinder retract), both the rodside pressure and pump pressure begin to oscillate together. This could potentially destabilize other functions if they were being used.

One possible method to deal with this problem would be to design a robust controller that accounted for variation in the system's coupled dynamics. An example of applying linear MIMO robust control to

complex hydraulic system is presented in Zhang et al. (2002). In comparison, the strategy utilized in this paper aims to decouple the pump pressure from the port pressures of the proportional flow valves. One way to nearly eliminate part of this coupling is to use pressure compensators (Pettersson et al., 1996). As long as the pump pressure remains high enough, the pressure drop across the orifice receiving flow from the pump remains constant regardless of pump pressure. This removes the "-c_3" term from Eq. 18 and replaces the P_s-P_r in the denominators of c_2 and c_3 with a near constant pressure drop.

How the coupling between the port pressure driving the load-sense and the pump pressure is removed is discussed in Section 5. The first step is to replace the hydro-mechanical load-sensing system with an electro-proportional regulator.

4 Flow Limited Control

Another factor that can destabilize pump pressure under feedback control is the amount of flow being command by the proportional valves. This requires a flow limiting or flow allocating algorithm. This is because a minimal amount of flow needs to be bypassed through the pressure relief valve and pressure reducing valve in order for the relief valves to maintain system pressure. Bypass flow is the difference between the pump flow and the flow being diverted to the proportional valves. The relief valve can only regulate pressure if there is flow going through it.

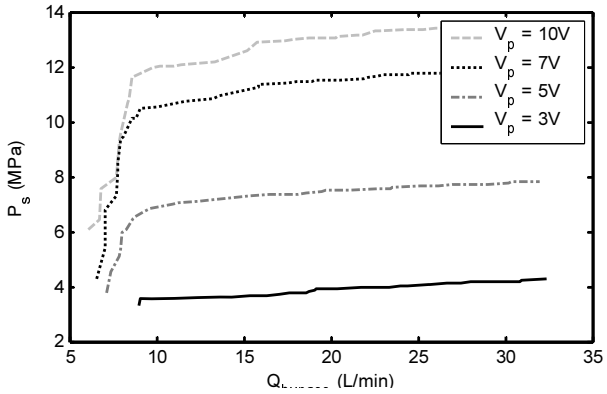

Fig. 8: *System pressure vs. bypass flow for constant pressure valve inputs*

Typically feedback control is not used to control mobile equipment. This means that if more flow is commanded than what is available, the flow will naturally be sent to the lower pressure circuits and nothing bad happens. With position based feedback control, the cylinder being starved of flow will slow down even as input or commanded flow to that cylinder increases. This causes the proportional valve to create a large metering orifice. Then once pump pressure is able to build up this cylinder would jump due to the large metering orifice and a sudden increase in pump pressure. If the pump pressure was being controlled using a load-sensing scheme, this sudden motion would cause a jump in port pressure that would be fed in the pump pressure via the load-sensing network.

In Fig. 8 the pressure relief valve does a good job of maintaining system pressure for a given input at bypass flow above 10 L/min (2.6 GPM). Below this flow, the pressure drops off sharply. This means that flow allocated to the actuators must be limited in order to assure the pressure regulator can work properly. While the results in Fig. 8 use the electro-proportional relief valve, the same is also true using either the hydro-mechanical load-sensing or constant pressure schemes. Even in an ideal case, the total flow being sent to the actuators could only match and not exceed the flow coming from the pump.

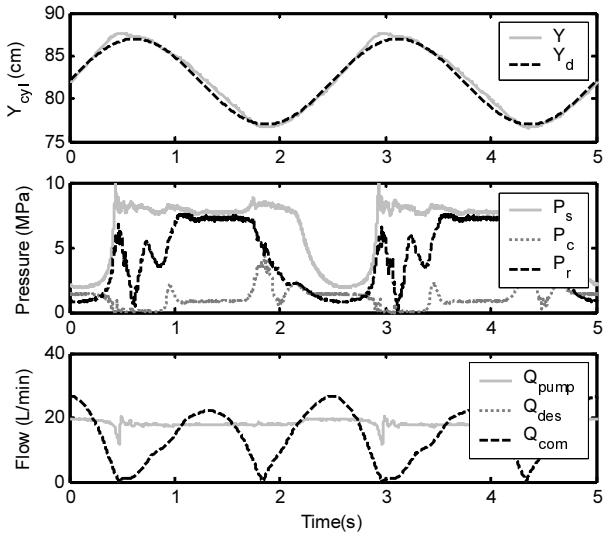

Fig. 9: *Constant system pressure command with low pump flow and no flow limiter. Here $Q_{des} = Q_{com}$*

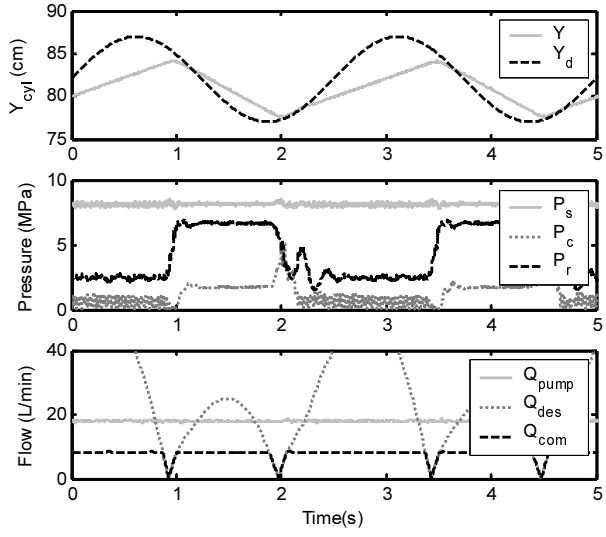

Fig. 10: *Constant system pressure command with low pump flow and flow limited motion*

The need for this type of flow limiting control is demonstrated by the boom cycles in Fig. 9. Y and Y_d are the actual and desired cylinder lengths. P_s, P_c and P_r are system, capside and rodside pressures. Q_{pump}, Q_{des} and Q_{com} are pump flow, desired cylinder flow and commanded cylinder flow. Note that without any limitation

on commanded flow, $Q_{des} = Q_{com}$ in Fig. 9. While the cylinder is retracting (boom rising) pressure must be maintained in order to overcome gravity. Since the constant pressure scheme is being used, the pressure should stay constant. When the cylinder is extending (boom lowering) pump pressure drops to less than half of the commanded value. This is not a problem for single degree-of-freedom motion; however, this is problematic if another degree-of-freedom requires this pressure and the boom motion is bleeding off the flow/pressure. A solution to this problem is to limit the total flow being sent to the cylinders. This is shown in Fig. 10. Tracking accuracy is greatly reduced since this limits cylinder velocity, but note the improved pressure regulation. Note that the poor tracking accuracy is exaggerated by the fact that the pump flow is very low in both of the cases shown in Figs. 9 and 10.

The end goal is to achieve a smooth and responsive multi-degree-of-freedom control using a haptic manipulator. Being able to maintain system pressure is necessary to achieve this goal. Limiting flow does cause the response to deviate from the desired command coming from the haptic interface. However, it is better to proportionally scale back all the commands and maintain smooth motion than allow system pressure to oscillate as the bypass flow dips below the critical value. Proportionally scaling back all the flow commands guarantees that the direction of the bucket's motion is maintained even if the speed is reduced.

5 Control of Pump Pressure

Originally the pump pressure was controlled using a hydro-mechanical load-sensing pressure valve. In principle this type of system works the same as a typical load-sensing system where pressure is fed back to control the flow of a variable displacement pumps. For a review of work on load-sensing systems see Wu et al. (2005). In this system, the pressure relief valve maintains a pressure margin between the system pressure and the highest pressure of the ports receiving flow from the pump. This pressure feedback is triggered by the position of the spools and a series of shuttle valves picks the highest pressure (Fig. 2).

As discussed in Section 3.3, the primary draw back is that the system is always coupled to one of the port pressures. This means that oscillation in one function is fed into the other functions. This also introduces complex dynamic interactions that can be driven unstable by feedback control. Another draw back is that at times the PVES spool control modules shown in Fig. 3 is starved of pressure. In addition to supplying the pressure being used by the proportional spools, it also supplies pressure to a reducing valve that regulates pressure going to the PVES modules. When this happens the spools cannot be moved as fast and the dynamics slow down. This compounds the delay associated with the spools moving through the dead-zone region.

One solution is to use a relief valve with a constant pressure setting. While this solution improves the dynamics response of the system it does so at the expense of efficiency and system temperature. An alternative is to use an electro-proportional relief valve. This enables the controller to decouple these states while still using the port pressure information to set the pump pressure. The merit of such a strategy is motivated by Section 3.3.

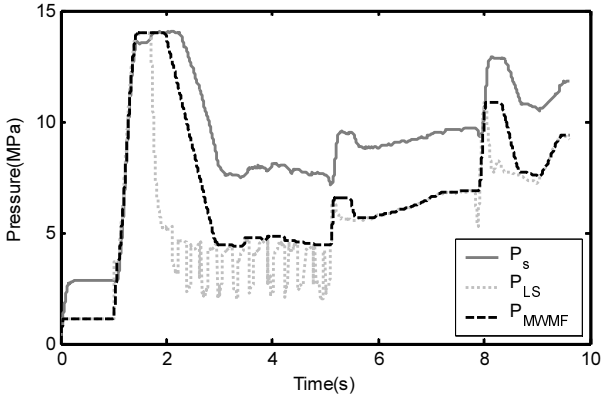

Fig. 11: *The dotted line is the original load-sense pressure signal generated from the port pressures receiving flow. Applying the Moving-Window-Max-Filter (MWMF) to this signal removes the oscillations (dashed line). The solid line is the resulting system pressure*

The method presented here uses a Moving-Window-Max-Filter (MWMF) to achieve the seemingly conflicting goals of using port pressures to control pump pressure while dynamically decoupling these states.

$$P_{\mathrm{MWMF}}(k) = \max\left\{P_{\mathrm{LS}}(k), \cdots, P_{\mathrm{LS}}(k-N)\right\} \tag{24}$$

The P_{LS} in Eq. 24 is the same as in Eq. 7; however, it is calculated electronically in the controller so the time constant is essentially zero since the sampling time is 1000 Hz. In addition, the switch that sets P_{LSi} equal to P_c, *0* or P_r is triggered by the desired flow, not the position of the spool. This means that pressure is building as the spool moves through the dead-band region. Computational resources including memory and comparisons can be minimized by splitting the window into subintervals. When the latest subinterval is full the oldest subinterval is dropped and a new one is started. This causes the exact length of the window to vary. The important thing is to always have the filter window wider than the period of any system oscillations.

Since it is a max function the high frequency component of an increase in desired pressure is not filtered out. However, if the port pressure driving the pump oscillates then the MWMF holds the desired pump pressure at the crest of the oscillation. Even though the load-sense pressure is oscillating, the MWMF removes most of the oscillations in the load-sense pressure from the system pressure. This is demonstrated in Fig. 11. A rate limiter is also used when the pressure is decreased. The downside is that pressure is held higher longer than it is actually needed. However, this is an acceptable compromise given that this enables the information to be used to vary the pressure. Figure 8 demonstrates that above a minimum bypass flow, the pressure primarily depends on input voltage. The pressure does increase a

little with additional bypass flow. This is likely due to flow forces (Manring, 2005) changing the force balance of the spool.

Data of pressure valve voltage versus pump pressure and bypass flow is used to create a three dimensional map. This three dimensional map is represented using a neural network that is trained off-line. The inputs to the network are system pressure and bypass flow and the output is the voltage. The bypass flow is the difference between the pump flow which is measured and the flow being diverted to the proportional valves. Flow is measured using a HYDAC EVS 3100-1 impeller type flow meter with a range of 6 - 60 L/min. Due to the engine speed range of the tractor and the constant displacement pump, the pump flow will stay between 15 - 35 L/min. The time constant of this flow meter is on the order of 50 ms. Since the data used to train the neural network is steady-state data, the time constant of the flow is not a factor. Even though bypass flow can be estimated, it is not used in the algorithm that calculates the pressure valve input because pressure spikes are fed through the flow meter. Doing so has a chaotic and destabilizing affect on the pressure control. Instead it is always assumed that only the minimum bypass flow set by the flow limiting control algorithm is passing through the relief valve. This still guarantees that the pump pressure is not lower than required.

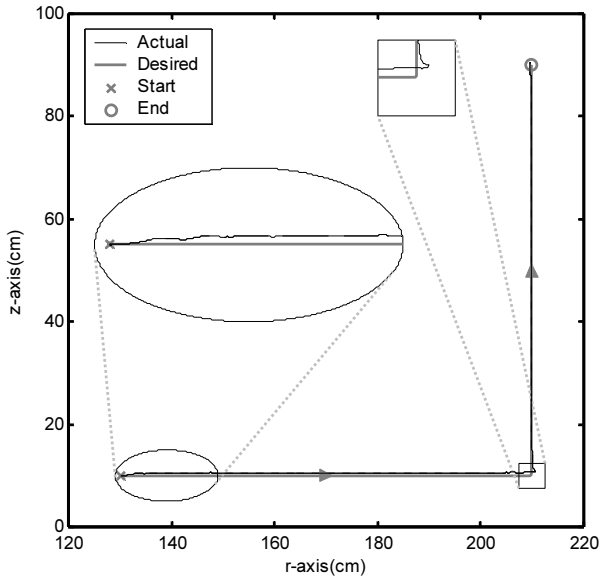

Fig. 12: *The trajectory is described in the workspace of the backhoe. Since the absolute bucket angle, φ, is held constant, the boom, stick and bucket must all work together*

The effectiveness of the MWMF is demonstrated using the trajectory in Fig. 12. The trajectory is a right angle path in the *r-z* plane in the workspace of the backhoe. The coordinates *r* and *z* are cylindrical coordinates that describe the motion of the wrist of the bucket relative to a reference frame located on the swing axis. These cylindrical coordinates *r* and *z* as well as the bucket angle, φ, and the cylinder length variables y_{c2}, y_{c3} and y_{c4} are defined graphically in Fig. 6. Since this desired path is described using task-space variables (*r*, *z* and φ), they must be mapped to joint-space variables and then to cylinder-space variables (y_{c2}, y_{c3} and y_{c4}). Details on these mappings are presented in Kontz and Book (2006). The bucket angle, φ, is maintained at a constant angle measured from the horizontal plane. The swing is not used. This motion requires the boom, stick and bucket to move at the same time. Pressure compensators are used and the desired flow command is generated using the following control law.

$$Q = A_{c(r)}\left(\dot{x}_d + k_p\left(x_d - x_c\right)\right) \tag{25}$$

The proportional feedback gain is *5* and the time derivative of the desired position is a feedforward term which is a partial plant inversion. The effect of the MWMF is shown in Fig. 13 which shows data corresponding to the sharp change in direction in Fig. 12. All three relevant cylinder lengths are shown. The pump pressure, P_s, and the two port pressures driving the electronic load-sense are shown. Before Y_2 starts to retract around 15.4 seconds, P_{r3} is driving the load-sense and at this time the pressure driving the load-sense changes to P_{r2}. Due to the sharp change in direction, P_{r2} is oscillating after this transition. However, due to the MWMF this oscillation is not sent to the valve controlling P_s. It can be seen in the blown up box in Fig. 12, that the motion of the backhoe overshoots, but is critically damped.

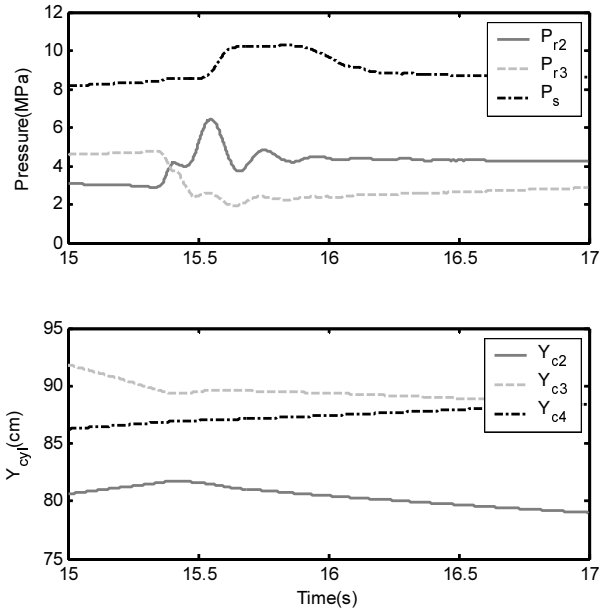

Fig. 13: *Cylinder position and pressure as the backhoe changes direction in Fig. 12. Only the two port pressures driving the electronic load-sense are shown in the plot with pump pressure, P_s.*

This demonstrates the effectiveness of the MWMF which is enabled by the flexibility of the electro-proportional relief valve. In comparison, pump pressure shown in Fig. 7 has sustained oscillation in pump pressure, P_s, for a single degree of freedom sinusoidal trajectory. While Figs. 12 and 13 show a sharp change in direction using three cylinders simultaneously there is no resulting oscillation in pump pressure. What this

means is that the electronic load-sensing scheme is able to capture the strength of both the hydro-mechanical load-sensing scheme and the hydro-mechanical constant pressure scheme. It allows pump pressure to follow the demands of system without the oscillations caused by the coupling of the port pressure and pump pressure in the hydro-mechanical load-sensing scheme.

6 Conclusions

Several reasons for using an electronic load-sensing pressure control strategy are presented. Using this type of pressure regulation scheme allows pressure to be built up as the spool moves through the dead-zone and raises the minimum system pressure to ensure that the spool control stage is always properly pressurized. This improves the overall responsiveness of the system. Combining the cylinder velocity control with a flow limiting algorithm is also necessary. If the total flow being sent to the actuators is too much, the pressure regulator can not maintain system pressure. This results in oscillations in the system pressure and ultimately jerky motion.

Using an electrical load-sensing scheme allows the pump pressure to be varied for efficiency while not compromising system stability. A moving-window-max-filter is presented. The max filter does not introduce lag while pressure is increasing. This means that it does not slow down pressure build up in the pump. However, it can remove oscillation in the desired pressure up to the period of the filter. Using a pressure compensator on the proportional valve helps decouple the pump pressure from oscillations in the port pressures being used to dictate the pump pressure in the load-sensing scheme. While the pump pressure is held high for a slightly longer period of time, it enables the pressure to be varied without compromising system stability.

Decoupling the pump pressure states from the flow states is important to the overall goals of this project which is to apply coordinated motion and haptic feedback to backhoes/excavators. This means that additional position and force loops can be added without exciting dynamic interactions between the pump pressure states and the states of the proportional valves. In a more general frame work, this decoupling strategy could be applied to any load-sensing system that was being controlled under feedback control.

Nomenclature

$\mathbf{A}$	State matrix	[na]
A_o	Orifice area	[m^2]
A_c	Cap (head) end area	[m^2]
A_r	Rod end area	[m^2]
$\boldsymbol{B}$	Input matrix	[na]
B_e	Effective bulk modulus	[Pa]
b_v	Damping coefficient	[N·s/m]
C_d	Discharge coefficient	[]
F_c	Cylinder force	[N]
F_{coul}	Coulomb friction force	[N]
g	Gravity constant	[m/s^2]
G	Gravity dynamic term	[N·m]
J	Inertia term	[kg·m^2]
k_p	Position P-gain	[N/m]
K_q	Orifice coefficient function	[$m^3/(s\sqrt{(Pa)})$]
KE	Kinetic energy	[J]
k_{sp}	Non-zero slope of K_{sp}	[$m^3/(s\sqrt{(Pa)})$]
l	Distance to centroid	[m]
m	Mass	[kg]
m_{eq}	Equivalent cylinder mass	[kg]
r	Cylindrical coordinate	[m]
P	Pressure	[Pa]
P_c	Cap end pressure	[Pa]
P_{LS}	Load-sense Pressure	[Pa]
P_{margin}	Pressure margin	[Pa]
P_r	Rod end pressure	[Pa]
P_s	System or pump pressure	[Pa]
ΔP	Pressure drop	[Pa]
Q	Flow	[m^3/s]
Q_c	Flow to cap end	[m^3/s]
Q_r	Flow to rod end	[m^3/s]
s	Laplace variable	[]
V_c	Oil volume on capside	[m^3]
V_{in}	Input voltage	[V]
V_r	Oil volume on rodside	[m^3]
$\boldsymbol{X}$	State vector	[na]
x_c	Cylinder position	[m]
x_d	Desired cylinder position	[m]
x_{sp}	Spool position	[m]
y_c	Cylinder displacement	[m]
z	Cylindrical coordinate	[m]
γ	Angle to centroid	[rad]
ζ	Damping ratio	[]
ρ	Density	[kg/m^3]
θ	Joint angle	[rad/s]
τ	Net torque input	[N·m]
φ	Absolute bucket angle	[rad]
τ_{LS}	Time constant of load-sense	[s]
τ_{Ps}	Time constant of P_s	[s]
ω_n	Main spool frequency	[rad/s]

Acknowledgements

This work is partially supported through HUSCO International, John Deere and the other supporting companies of the Fluid Power and Motion Control Center of Georgia Tech.

References

Fortgang, J. D., **George, L. E.** and **Book, W. J.** 2002. Practical implementation of a dead zone inverse on a hydraulic wrist. *Intl. Mech. Engr. Congr. Expo.*, FPST-Vol 9, ASME New Orleans, LA, 149-155.

Frankel, J. G. 2004. *Development of a Haptic Backhoe Testbed.* M. S. Thesis. G. W. Woodruff School of Mechanical Engineering. Georgia Institute of Technology.

Ha, B. Q., **Santos, M.**, **Nguyen, Q.**, **Rye, D.** and **Durrant-Whyte, H.** 2002. Robotic excavation in construction automation. *IEEE Robotics and Automation Magazine,* 9(1), 20-28.

Kappi, T. J. and **Ellman, A. U.** 2000. Analytical method for defining pressure compensator dynamics. *Intl. Mech. Engr. Congr. Expo.*, FPST-Vol 7, ASME, Orlando, FL, 121-125.

Kontz, M. E., **Beckwith, J.** and **Book, W. J.** 2005a. Evaluation of a teleoperated haptic forklift. *Intl. Conf. on Adv. Intelligent Mechatronics*, IEEE/ASME, Monterey, CA, 295-300.

Kontz, M. E., **Huggins, J. D.**, **Book, W. J.** and **Frankel, J. G.** 2005b. Improved Control of Open-center Systems for Haptics Applications. *Intl. Mech. Engr. Congr. Expo.*, DSC-Vol 74-1A, ASME, Orlando, FL, 823-831.

Kontz, M. E. and **Book, W. J.** 2006. Kinematic Analysis of Backhoes/Excavators for Closed-loop Coordinated Control. *Proc. Intl. Symp. Robot Control*, Bologna, Italy.

Kontz, M. E. and **Book, W. J.** 2007. Flow Control for Coordinated Motion and Haptic Feedback. *Intl. Journal Fluid Power (submitted)*.

Krishnaswamy, K. and **Li, P. Y.** 2006. Bond graph based approach to passive teleoperation of a hydraulic backhoe. *ASME J. Dyn. Syst. Meas. and Control,* 128(1), 176-85.

Lee, S. -U. and **Chang, P. H.** 2001. Control of a heavy-duty robotic excavator using time delay control with switching action with integral sliding surface. *Proc. Intl. Conf. on Robotics and Automation*, IEEE, Seoul, South Korea, 3955-60.

Liu, S. and **Yao, B.** 2004. Programmable valves: a solution to bypass deadband problem of electro-hydraulic systems. *Proc. American Control Conf.*, Boston, MA, 4438-43.

Manring, N. D. 2005. *Hydraulic Control Systems.* Hoboken, NJ. John Wiley and Sons, Inc.

Massie, T. H. and **Salisbury, K. J.** 1994. PHANToM haptic interface: a device for probing virtual objects. *Intl. Mech. Engr. Congr. Expo.*, DSC-Vol 55-1, ASME, Chicago, IL, 295-299.

Merritt, H. E. 1967. *Hydraulic control systems.* New York. Wiley.

Pettersson, H., **Krus, P.**, **Jansson, A.** and **Palmberg, J. -O.** 1996. The Design of Pressure Compensators for Load Sensing Hydraulic Systems. *Proc. Int. Conf. Control*, London, UK, 1456-1461.

Rosenberg, L. B. 1993. Virtual fixtures: perceptual tools for telerobotic manipulation. *Proc. Virtual Reality Annual Intl. Symp.*, IEEE, Seattle, WA**,** 76-82.

Salcudean, S. E., **Hashtrudi-Zaad, K.**, **Tafazoli, S.**, **Dimaio, S. P.** and **Reboulet, C.** 1999. Bilateral matched impedance teleoperation with application to excavator control. *IEEE Control Systems Magazine,* 19(6), 29-37.

Stentz, A., **Bares, J.**, **Singh, S.** and **Rowe, P.** 1998. A robotic excavator for autonomous truck loading. *Proc. Intl. Conf. on Intelligent Robots and Systems.*, IEEE/RSJ Victoria, BC, Canada, 1885-93.

Tafazoli, S., **Peussa, P.**, **Lawrence, P. D.**, **Salcudean, S. E.** and **De Silva, C. W.** 1996. Differential PWM Operated Solenoid Valves in the Pilot Stage of Mini Excavators: Modeling and Identification. *Intl. Mech. Engr. Congr. Expo.*, FPST-Vol. 3, ASME, Atlanta, GA, 93-99.

Tafazoli, S., **Salcudean, S. E.**, **Hashtrudi-Zaad, K. and Lawrence, P. D.** 2002. Impedance control of a teleoperated excavator. *IEEE Trans. Control Systems Technology,* 10(3), 355-367.

Taware, A., **Tao, G.** and **Teolis, C.** 2002. Design and analysis of a hybrid control scheme for sandwich nonsmooth nonlinear systems. *IEEE Tran. Automatic Control,* 47(1), 145-150.

Vaha, P. K. and **Skibniewski, M. J.** 1993. Cognitive force control of excavators. *J. Aerospace Engineering,* 6(2), 159-166.

Wallersteiner, U., **Stager, P.** and **Lawrence, P.** 1988. A human factors evaluation of teleoperator hand controllers. *Proc. Intl. Symp. Teleoperation and Control*, Bristol, UK, 291-6.

Wallersteiner, U., **Lawrence, P.** and **Sauder, B.** 1993. Human factors evaluation of two different machine control systems for log loaders. *Ergonomics,* 36(8), 927-934.

Wu, D., **Schoenau, G.**, **Burton, R.** and **Bitnet, D.** 2005. Model and Experimental Validation of a Load Sensing System. *Intl. Journal Fluid Power,* 6(3), 5-18.

Zhang, R., **Alleyne, A.** and **Prasetiawan, E.** 2002. Modeling and H2/H-infity MIMO Control of an Earthmoving Vehicle Powertrain. *ASME J. Dyn. Syst. Meas. and Control,* 124(4), 625-636.

Matthew E. Kontz
He received a B. S. E. from Walla Walla College in 2001 and a M. S. M. E in 2002 from the Georgia Institute of Technology. By the end of 2007, he plans to begin a career at Caterpillar and receive both a M. S. in Electrical Engineering and Ph. D. in Mechanical Engineering from Georgia Tech. His graduate research has centered on haptic control of hydraulic machinery. Prior industrial experience includes internships at Honeywell and Caterpillar and independent consulting for Ross Controls. He was the primary author on the paper receiving the 2005 ASME IMECE FPST Division Best Paper Award.

Wayne J. Book
After he received his Ph. D. degree in mechanical engineering from the Massachusetts Institute of Technology in 1974, Wayne Book joined the faculty of Mechanical Engineering at the Georgia Institute of Technology. He is currently the HUSCO/Ramirez Distinguished Professor in Fluid Power and Motion Control. His research includes the design, dynamics and control of high speed, lightweight motion systems, robotics, fluid power and haptics. He is a Fellow of both the ASME and IEEE, and received Georgia Tech's award for Outstanding Faculty Leadership for development of Graduate Research Assistants in 1987, and an ASME Dedicated Service Award in 2003 and the ASME DSCD Leadership Award in 2004.